Emergent Materials (2020) 3:857–870
https://doi.org/10.1007/s42247-020-00126-w

ORIGINAL ARTICLE

Removal of copper ions from aqueous solution using NaOH-treated rice husk

Shagufta Zafar[1,2] · Muhammad Imran Khan[3] · Mushtaq Hussain Lashari[4] · Majeda Khraisheh[5] · Fares Almomani[5] · Muhammad Latif Mirza[2] · Nasir Khalid[6]

Received: 24 December 2019 / Accepted: 23 September 2020 / Published online: 12 October 2020

Abstract

The present study investigates the removal of copper ions (Cu (II)) from aqueous solution using chemically treated rice husk (TRH). The chemical treatment was carried out using NaOH solution and the effect of contact time (t_c), adsorbent dosage (D_{ad}), initial Cu (II) concentration ($[Cu]_i$), and temperature (T) on the percentage removals of Cu (II) ($\%R_{Cu}$) were investigated. Different analytical techniques (FTIR, SEM, and EDX) were used to confirm the adsorption (*ads*) of Cu (II) onto the TRH. The *ads* kinetics was tested against pseudo-first-order (PFO) and pseudo-second-order (PSO) models as well as Langmuir and Freundlich isotherms. Treating RH with NaOH altered the surface and functional groups, and on the surface of RH, the ionic ligands with high electro-attraction to Cu increased and thus improved the removal efficiency. The $\%R_{Cu}$ decreased by increasing the $[Cu]_i$ and increased by increasing the c_t, D_{ad}, and T. Up to 97% Cu removal was achieved in c_t of 30 min using D_{ad} of 0.3 g $[Cu]_i$ of 25 mg L^{-1} and T = 280 K. The *ads* of Cu on TRH is endothermic, spontaneous, follows Langmuir isotherms, and exhibited a PSO kinetics. Moreover, the TRH was successfully regenerated and used for further adsorption cycles using 1 M HNO_3.

Keywords Adsorption · Desorption · Copper ion · Treated rice husk · Kinetics · Isotherms · Thermodynamics

1 Introduction

Water contamination with heavy metals is considered a global issue and caused great concern worldwide [7]. Toxic metal ions can be introduced to the water body from different industrial effluents such as metal plating facilities, mining operations, fertilizer industries, tanneries, batteries, paper industries, and pesticides. Heavy metals are extremely toxic, non-biodegradable, and do not undergo thermal degradation, and once they enter the food chain, they can accumulate at low concentrations in the living organisms [26, 62, 104, 105]. Therefore it has become imperative to develop a treatment process for the removal of such wastes. Different studies have reported that heavy metals such as lead, zinc, cadmium, chromium, and copper are very toxic elements [2, 4, 7, 8]. Drinking water containing copper exceeding the permissible limit for a long period leads to irreversible kidney or liver damage as well as headaches, hair loss, and increased heart rate, and in some cases might cause brain dysfunction, depression, and schizophrenia [19, 61]. According to the World Health Organization

Shagufta Zafar and Muhammad Imran Khan contributed equally to this work.

✉ Fares Almomani
falmomani@qu.edu.qa

[1] Department of Chemistry, The Government Sadiq College Women University, Bahawalpur 63000, Pakistan

[2] Department of Chemistry, The Islamia University of Bahawalpur, Bahawalpur, Pakistan

[3] School of Energy and Power Engineering, Xi'an Jiaotong University, 28 West Xianning Road, Xi'an 710049, Shaanxi, People's Republic of China

[4] Department of Zoology, The Islamia University of Bahawalpur, Bahawalpur 63100, Pakistan

[5] Department of Chemical Engineering, College of Engineering, Qatar University, Doha, Qatar

[6] Chemistry Division, Pakistan Institute of Nuclear Science and Technology, PO Nilore, Islamabad, Pakistan

(WHO) and Environmental Protection Agency (EPA) guidelines, the maximum allowable concentration of Cu (II) in drinking water is 1.3 and 2.0 mg L^{-1}, respectively [11, 82, 100]. Therefore, the treatment of wastewater containing Cu (II) is crucial in the field of environmental protection [69, 86].

Conventional methods including coagulation, chemical precipitation, ion exchange, adsorption, membrane separation, reverse osmosis, oxidation, evaporation, electro-flotation, and solvent extraction were successfully employed for the removal of heavy metals [73, 96]. However, most of these methods have some disadvantages such as complicated treatment process, high cost, and high energy demand. Among these methods, adsorption (*ads*) is considered as the most widely used method due to high performance, economical feasibility, and simple application [17, 27, 36, 52, 89, 92]. In general, activated carbon is the most commonly used adsorbent for the removal of heavy metals from industrial wastewater due to its high surface area, microporous structure, and high adsorption capacity. However, it is expensive with relatively high operating costs and there is a need for regeneration after each *ads* cycle [5]. Hence, there is a growing demand to find efficient, low-cost, and locally available adsorbents to be employed for the removal of copper from wastewater. Natural adsorbents such as sugarbeet pulp [3, 16], peanut hull [117], *Cinnamomum camphora* leaf powder [17], litter of poplar forests [22], lentil shell [10], wheat shell [9, 10], rice shell [10], almond shell [71], herbaceous peat [28], *Tectona grandis* L.f. leaf powder [85], base treated rubber leaves [75], pine cone powder [79], spent grain [65], tree fern [32], groundnut shells [94], pretreated *Aspergillus niger* [72], cedar sawdust [21], crushed brick [21, 102], and sawdust [56] have attracted many researchers and employed for heavy metal removals due to their low cost, high availability, and simple regeneration process.

Different mechanisms were used to explain the removal of heavy metals via natural adsorbents including micro-precipitation, chelation, complexation, ion exchange, and physical adsorption [13, 18]. The *ads* is related to the attraction force between the functional groups with a negative charge on the surface of the adsorbents with the positively charged metals [88, 91]. Accordingly, a treatment process that can enhance and improve the negative surface charge would significantly increase heavy metal removal performance. Wang et al. [107] enhanced the metal removal of uranium using rice stems by applying alkalinity treatment. Teixeira Tarley et al. [99] showed that applying chemical treatment for rice husk improved significantly the *ads* capacity of different metal cations. He and Chen [29] showed that the organic functional groups on the surface of bio-sorbents play a leading role in the removal of HM. Luo et al. [67] improved the heavy metal removal by brown algae *Laminaria japonica* via chemical crosslinking modification using epichlorohydrin potassium permanganate (PC).

Although different research works were published on the use of natural adsorbents for heavy metal removal, factors affecting the improvement of the *ads* capacity after chemical treatment still need further investigation. In addition, there is a lack of knowledge regarding the effect of surface properties and functional groups on the performance and capacity of natural adsorbents for the removal of metals from wastewater. Moreover, the kinetics and mechanisms of the *ads* process remain challenges due to the selectivity and complicity of the system.

Given that Pakistan is one of the world's major producers of rice (5.2 million tons annually), rice husk (RH) which forms 20–23% of the whole rice grain is produced in huge amounts and is considered as unwanted waste material that poses a disposal problem for mill owners [63, 112, 113]. Due to its unique composition including proteins, cellulose, hemicellulose, and lignin that mainly have hydroxyl and carboxyl functional groups, it can be possible natural adsorbents for the removal of heavy metals from wastewater [20, 58–60, 78, 90]. It is imperative that the use of RH for heavy metal removal required treatment to rearrange and organize such a functional group on the surface to enhance the removal efficiency [99]. To the best of our knowledge, the *ads* of Cu (II) onto TRH has not been studied yet. Therefore, the present study reports on enhancing the *ads* efficiency of the RH by applying chemical treatment using NaOH as a low-cost and easy approach. The changes in surface morphology and the functional group as well as the improvements in the percentage removal of Cu (II) ($\%R_{Cu}$) were investigated. The thermodynamics, kinetics, and isotherms of the *ads* process were also explored. The study also evaluated the effects of different operational conditions including contact time (t_c), adsorbent dosage (D_{ad}), initial Cu (II) concentration ($[Cu]_i$), and temperature (T) on the percentage removal of Cu (II) ($\%R_{Cu}$). The feasibility of the Cu *ads* was enhanced by regenerating and reusing the TRH for several times.

2 Experimental

2.1 Adsorbent

The husk of basmati rice (botanical name *Oryza sativa*) was obtained from a rice mill in Punjab, Pakistan. All experimental works were conducted from the same batch to eliminate any effect of seasonal variation in the rice sample. The collected RH has a bulk density in the range 88–135 kg m^{-3} and contains 50% cellulose, 23–27% lignin, 15–20% silica, and 10–17% moisture. The stock husk samples were thoroughly washed with water to remove dust particles and were oven-dried at 80 °C until a constant weight was obtained. The dry husk was then stored in a pre-cleaned airtight container and used in the experiments.

The chemical treatment of RH was carried by mixing the dry samples with 1 N NaOH at a ratio of 1 g RH/20 ml NaOH at 35 ± 1 °C. Then, the RH was recovered by filtration through a 0.45-μm filter (Whatman, USA) and washed with distilled water (DW) until the pH of water reached pH 7 ± 0.5 to remove any traces of NaOH remaining in the RH. The RH was then dried as before (80 °C to reach constant weight), denoted as TRH and used in experiments. The chemical measurements of the TRH using neutron activation analysis (NAA, DF-5703(A); DFMC, China) and atomic sorption spectrometry (AAS, WFX220AB; Qualitest, USA) techniques showed the presence of traces elements (Na, K, Pb, and Fe, in mg $g^{-}1$) and 18.27 ± 0.62% of the TRH as silica.

2.2 Reagents

Chemicals used in the present study are analytical grades purchased from Sigma-Aldrich and used as received. For thermodynamic investigations, the temperature of solutions was controlled at ±0.1°C by immersing the test tubes in a water bath (Gallenkamp thermo stirrer, UK).

2.3 Batch adsorption

Adsorption experiments were carried out using a shaker (Gefellschaft Fur 978, Germany) and temperature-controlled (Gefellschaft Funn 1003, Germany) set up. The pH of the water samples was measured using a pH meter (Oiron 520; Thermo Scientific, USA). The concentrations of Cu (II) was measured using a model AA 100, inductively coupled plasma-atomic emission spectrometry (ICP) (Perkin-Elmer, USA). A four-digit analytical balance with a precision of ±0.0001 mg (Sartorius, CP324-S, USA) was used in weighing samples.

All *ads* tests were carried out in a batch mode under controlled pH and temperature. A series of 25-cm^3 secured cap tubes filled with 4 cm^3 of the standard acid solution, a fixed amount of stock radiotracer, and a specific concentration of copper (25 to 200 mg L^{-1}) were mixed with a specific dose of adsorbent (0.05 to 0.6 g). The mixture was agitated in a wrist-action mechanical shaker (Vibromatic, USA) at 500 rpm for 30 min to reach equilibrium. Then, the agitator was stopped, and the solution was centrifuged at 5000 rpm for 30 min to separate solid adsorbent from water. The supernatant was separated from the solid adsorbent, the concentration of Cu (II) in the solution was determined, and percentage removal of Cu (II) ($\%R_{Cu}$) was calculated using Eq. (1). Control tests were performed at different pH for samples containing heavy metals alone to evaluate the percentage removal of heavy metal by precipitation. The effect of temperature on the Cu removal was studied by repeating the tests at different temperatures 280.0 ± 1 to 335 ± 1 K.

$$\%R_{Cu} = \frac{[Cu]_i - [Cu]_f}{[Cu]_i} \times 100\% \quad (1)$$

where $[Cu]_i$ and $[Cu]_f$ are the initial and final concentrations of Cu (mg $L^{-}1$), respectively.

2.4 Kinetic study

The kinetic of the *ads* of Cu (II) onto TRH was tested against Lagergren's pseudo-first (PFO) [55], Eq. (2), and pseudo-second-order (PSO) [30, 31], Eq. (3), using IGOR Pro 6.1.2, Wave Metrices software.

$$\frac{dQ_t}{dt} = k_1 (Q_e - Q_t) \quad (2)$$

$$\frac{dQ_t}{dt} = k_2 (Q_e - Q_t)^2 \quad (3)$$

where Q_t is the amount of Cu (II) adsorbed on the TRH at any time t (mg $g^{-}1$), Q_e is the equilibrium amount of Cu (II) adsorbed on the TRH (mg g^{-1}), t is the time (min), k_1 (min^{-1}) and k_2 (g mg^{-1} min^{-1}) are the PFO and PSO rate constants, respectively. Equations (2) and (3) can be written in a linear form as per Eqs. ((Linear 4) and ((Linear 5) [15, 33, 83].

$$\log(Q_e - Q_t) = \log Q_e - \left(\frac{k_1}{2.303}\right) t \quad \text{(Linear4)}$$

$$\frac{t}{Q_t} = \frac{1}{k_2 Q_e^2} + \frac{t}{Q_e} \quad \text{(Linear5)}$$

Regression coefficient R^2, Eq. (6), and χ^2 test, Eq. (7), were used to compare the best fit of the kinetic model,

$$R^2 = \frac{\Sigma\left(Q_{t,cal} - \overline{Q}_{t,\exp}\right)^2}{\Sigma\left(Q_{t,cal} - \overline{Q}_{t,\exp}\right)^2 - \Sigma\left(Q_{t,cal} - Q_{t,\exp}\right)^2} \quad (6)$$

$$\chi^2 = \Sigma \frac{(Q_e - Q_{e,cal})^2}{Q_{e,cal}} \quad (7)$$

where $Q_{t,\exp}$ is experimental *ads* capacity at any time t (mg g^{-1}), $Q_{t,cal}$ is calculated *ads* capacity at any time t (mg g^{-1}), $\overline{Q}_{t,\exp}$ is average of the experimental *ads* capacity at any time (mg g^{-1}), and Q_e and $Q_{e,cal}$ are the experimental and calculated equilibrium *ads* capacity (mg g^{-1}), respectively.

2.5 Adsorption isotherms

For scale-up purposes, the *ads* process of Cu on TRH was tested against Langmuir (Eq. 8), Freundlich (Eq. 9), and Dubinin–Radushkevich isotherms.

$$\frac{[Cu]_e}{Q_e} = \frac{1}{Q_{max} K_L} + \frac{[Cu]_e}{Q_{max}} \quad (8)$$

$$\log q_e = \log K_f + \frac{1}{n}\log[Cu]_e \quad (9)$$

$$\ln q_e = \ln C_{\max} - \beta\varepsilon^2 \quad (10)$$

where $[Cu]_e$ is the equilibrium concentration of Cu(II) the solution (mol L^{-}1), Q_e is the equilibrium amount adsorbed on TRH per unit mass (mol g^{-1}), Q_{max} is the maximum *ads* capacity (mol g^{-1}), and K_L (L mol^{-1}) is related to the energy of adsorption, K_f and n are Freundlich constants, C_{max} (mol g^{-1}) is the maximum amount of Cu can be adsorbed onto TRH under the optimized experimental conditions, β is a constant related to adsorption energy, and ε (Polyanyi potential) = $RT\ln\left(1+\frac{1}{C_e}\right)$ where R is the universal gas constant (KJ mol^{-1} K^{-1}) and T is the absolute temperature (K).

2.6 Adsorption thermodynamic

The thermodynamic of the adsorption process was followed by the changes in Gibb's free energy (ΔG^o), enthalpy (ΔH^o), and entropy (ΔS^o) following Eqs. (11) and (12) [41, 43–45, 49, 50]:

$$\ln Kc = \frac{\Delta S^o}{R} - \frac{\Delta H^o}{RT} \quad (11)$$

$$\Delta G^o = \Delta H^o - T\Delta S^o \quad (12)$$

where K_c is the *equilibrium* constant, R is the general gas constant (8.31 J mol^{-1} K^{-1}), and T is the absolute temperature (K).

2.7 Characterization

FTIR spectra of virgin and Cu (II) loaded TRH were recorded by employing the attenuated total reflectance (ATR) technique with an FTIR spectrometer (Vector 22; Bruker) having a resolution of 2 cm^{-1} and a total spectral range of 4000–400 cm^{-}1. Field emission scanning electron microscope (FE-SEM, Sirion200; FEI Company, USA) was employed to study the morphology of virgin and Cu (II) loaded TRH. Similarly, energy-dispersive X-ray (EDX) analysis was used to prove the successful adsorption of Cu (II) onto TRH. The porosity of the TRH was measured using a porosimetry analyzer (Micromeritics Autopore IV 9500 V1.05). Tests were conducted using nitrogen adsorption–desorption isotherm (ADDE-ISO) at a pressure in the range of 0.1–20,000 psia.

2.8 Statistical analysis

The statistical significance of all the experimental results was evaluated using Student's paired *t* test. The test was conducted to investigate the significance of the results using one-way ANOVA (GraphPad Prism statistics software, version 7.04, USA). Only the experimental results that were statistically accepted at a significance level of 5% were used in the results and discussion section.

2.9 Recovery of Cu (II) and recycling the TRH

Attempts were made to recover the adsorbed Cu (II) from the TRH using hydrochloric, sulfuric, and nitric acid as desorbing media. The object is to recover the Cu and reuse the TRH many times for treating wastewater contaminated with Cu.

Desorption of Cu was conducted by mixing the TRH with 10 mL of acids for 30 min and then sonicating for 5 min. After that, the TRH was separated by filtration, washed with DW 10 times, dried, and reused for the consecutive adsorption–desorption process.

3 Results and discussion

3.1 Characterization of treated rice husk (TRH)

The FTIR spectrum of the RH is represented in Fig. 1a. The absorption peaks in the band 3400-3200 cm^{-1} were assigned to surface O-H stretching, whereas the peaks at 2921–2851

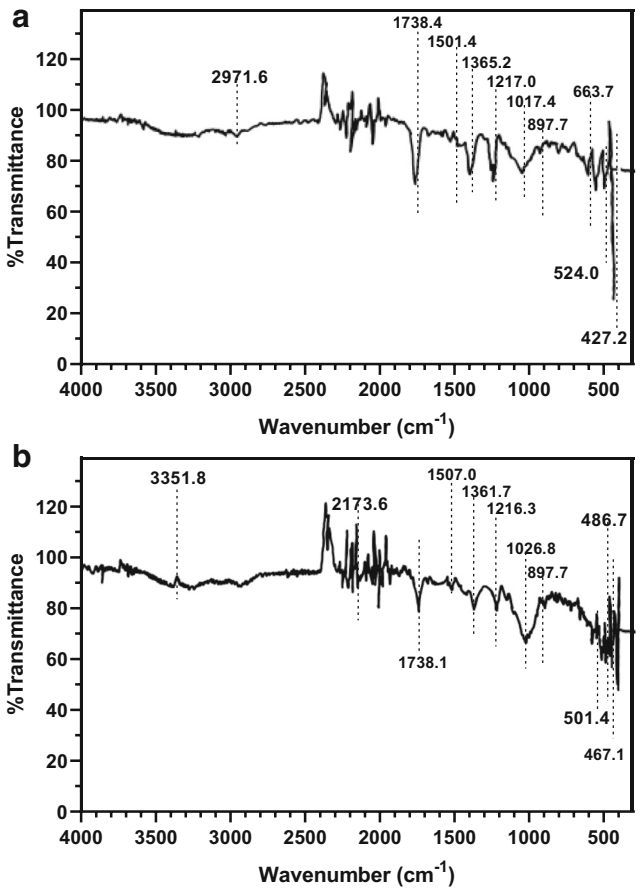

Fig. 1 FTIR spectrum of **a** virgin TRH and **b** Cu (II) loaded TRH

cm^{-1} correspond to the aliphatic stretching in the C-H bond. Other peaks at 1738.4, 1501.4, and 1365.2 cm^{-1} were associated with C=O stretching, OH bending of the adsorbed H_2O, and aliphatic C-H bending, respectively [38]. Other peaks in the range 1208–1230, 1367-1371, 1740, and 1029 cm^{-1} were associated with carboxyl group [37, 97].

Treating the RH with NaOH has changed the functional group on the surface of the RH as it is evident by the shift in the peak from 2971.6 to 3351.8 cm^{-1} and the peaks in the range 3173.8 to 1026.8 cm^{-1}. The absence of peaks related to non-conjugated carbonyl functional groups in the range 2750 to 2850 cm^{-1} indicated the hydrolyses of carbonyl groups during NaOH treatment. Furthermore, the peak at 1074.0 cm^{-1} corresponds to the anti-symmetric stretching vibration of Si-O, whereas at 476.2 cm^{-1} indicates the bending vibration of Si-O-Si bond [66, 97]; [111]. Measurements showed that NaOH treatment altered the surface functional groups of the TRH and increased the ionic ligands of carboxyl, phosphate, and amino groups that have high electro-attraction force with the positively charged Cu^{+2}. These conditions increased the TRH capacity to remove Cu^{+2} from the aqueous solution. Similar trends were observed by He and Chen [29] during the removal of heavy metals by algal biomass. As it was presented in the FTIR results, the chemical treatment showed an increase in the intensity of O-H, C-H, and C=O groups which have high ionic exchange capacity to uptake Cu from the solution [88].

In Fig. 1b, the FTIR spectra of Cu (II) loaded on TRH exhibited changes in the peak positions and relative intensities. The shifting of peaks to 1026.8 and 501.4 and decrease in intensity of 1738.1, 1507.0, 1361.7, and 1216.3 cm^{-1} were observed for TRH, which suggests that less stretching occurs due to the binding of Cu (II) with carboxyl and silanol groups present in rice husk. It was also observed that a new peak at 467 cm^{-1} associated with Si–O bending vibration has been observed after the adsorption of Cu (II) onto TRH. Marshall and Johns [70] showed that the treatment of soybean and cottonseed hulls improved sorption capacity for Zn(II) compared with the untreated materials due to the increase in galacturonic acid groups on the surface. Low et al. [64] observed that treatment with NaOH improved the sorption of spent grain. However, Xie et al. [109] indicated that it can dissolve biomass and destroy metal-binding sites. The FTIR analysis before and after the adsorption suggested that there is some sort of interaction among protonated –OH and Si–O groups of rice husk and Cu.

Figure 2 represents the SEM micrographs of TRH before and after the adsorption of Cu (II). The surface of rice husk was irregular and rough with many loops and humps. The pores can be classified according to their sizes. Primary micro-pores are less than 0.8 nm, secondary micro-pores are 0.8–2 nm, meso-pores are 2–50 nm, and macro-pores are 50 nm width in size. The determined pore size present on the surface TRH was 335–1220 nm confirming the macroporous structure of adsorbents (Fig. 2a, c). The SEM images (Fig. 2b, d) of TRH loaded with Cu (II) showed that the surface of adsorbent becomes smooth and occupied with Cu as a result of adsorption (see red circle in Fig. 2d). The radius of copper is 0.091 nm which was much smaller than the pore sizes of rice husk, so metal ions may be adsorbed through diffusion into pores. The capacity of Cu (II) *ads* onto TRH was increased from 1.919×10^{-5} to 9.168×10^{-5} mol g^{-1} because of the tremendous increase in the size and number of pores on TRH. The observed trend can be related to the changes in surface morphology due to disruption of the cross-linking between the metal ions and negatively charged chemical groups as confirmed by Florido et al. [24], Iqbal et al. [34], and Kızılkaya et al. [51] and evidenced by the increase surface *ads* of Cu.

Figure 3 presents the EDX analysis of the energy peak as a result of the *ads* of Cu (II). Results revealed the presence of Cu (II) onto adsorbent surfaces and copper peaks were present at different energy levels ranging from 0.750 to 8.80 keV confirming the successful *ads* of Cu (II) onto TRH.

3.2 Adsorption of Cu on treated rice husk (TRH)

3.2.1 Effect of contact time

Figure 4a shows that the $\%R_{Cu}$ increased from 35.4 to 95.5% as the t_c increased from 0 to 10 min, and then to 97.1% for c_t of 30 min. The observed trends suggest that the *ads* of Cu (II) on TRH was very fast initially for the first few minutes and there was no significant change in $\%R_{Cu}$ once the equilibrium was established. Therefore, there was no further significant increase in $\%R_{Cu}$ as the c_t increased. The obtained trends can be related to the existence of a large number of empty active sites onto TRH initially, which led to establishing an interaction between Cu (II) and *ads* sites on TRH. Once the active sites were occupied, the *ads* slowed down and $\%R_{Cu}$ decreased due to the movement of metal ions deep into interior pores of TRH. Based on the results from Fig. 4a, it can be concluded that the equilibration time for Cu (II) on TRH was only 15 min, which is a very short time compared with equilibration time for Ce (IV) [48, 113].

3.2.2 Effect of the adsorbent dosage (D_{ad})

Figure 4b presents the effect of the adsorbent dosage (D_{ad}) of TRH (0.05 to 0.6 g) onto the $\%R_{Cu}$ of Cu (II). The $\%R_{Cu}$ was enhanced from 18.2 to 97.8% by increasing the D_{ad} of the TRH from 0.05 up to 0.3 g, beyond which no significant enhancement in the $\%R_{Cu}$ was observed. An amount of 0.20 g of TRH was observed to be the optimum D_{ad} that generates maximum $\%R_{Cu}$ under the studied conditions.

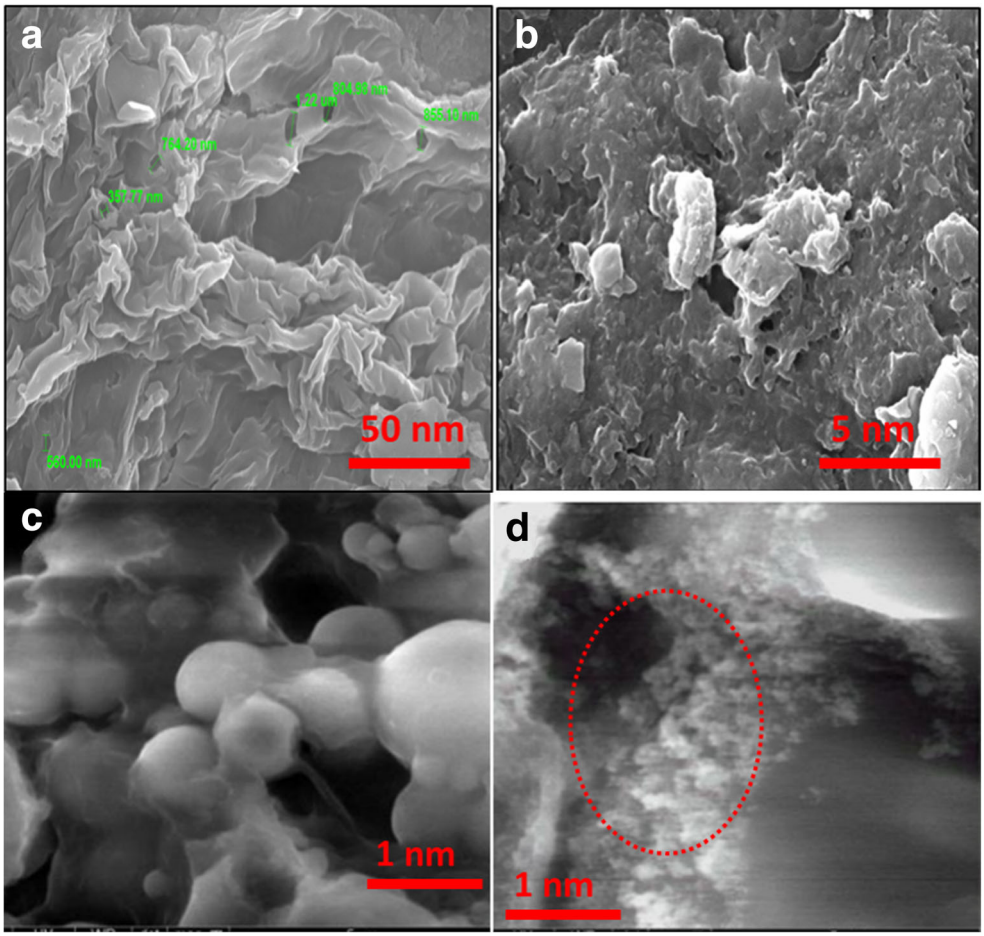

Fig. 2 SEM image of **a**, **c** virgin and **b**, **d** Cu (II) loaded TRH

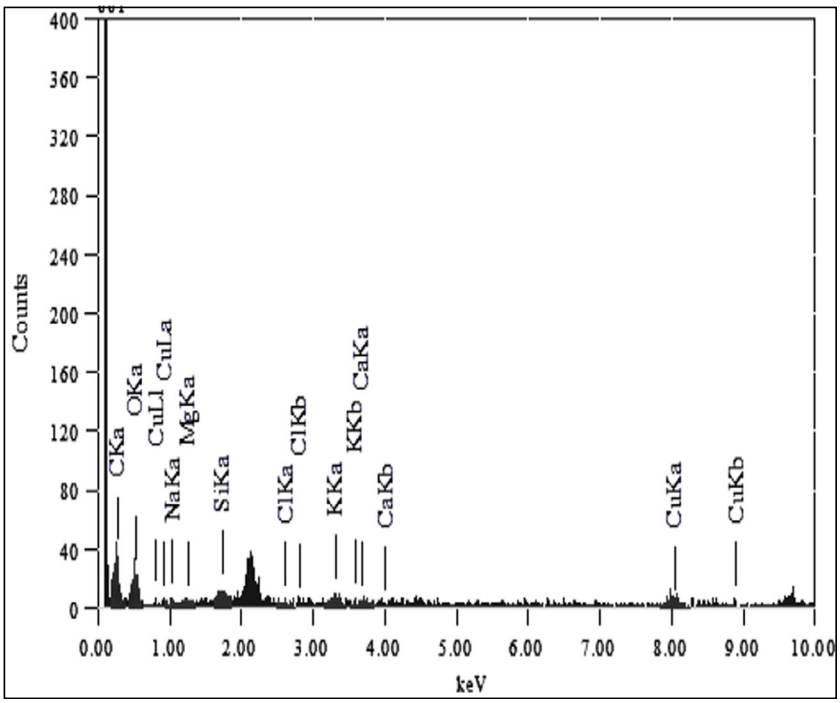

Fig. 3 Energy-dispersive X-ray image of Cu (II) loaded TRH

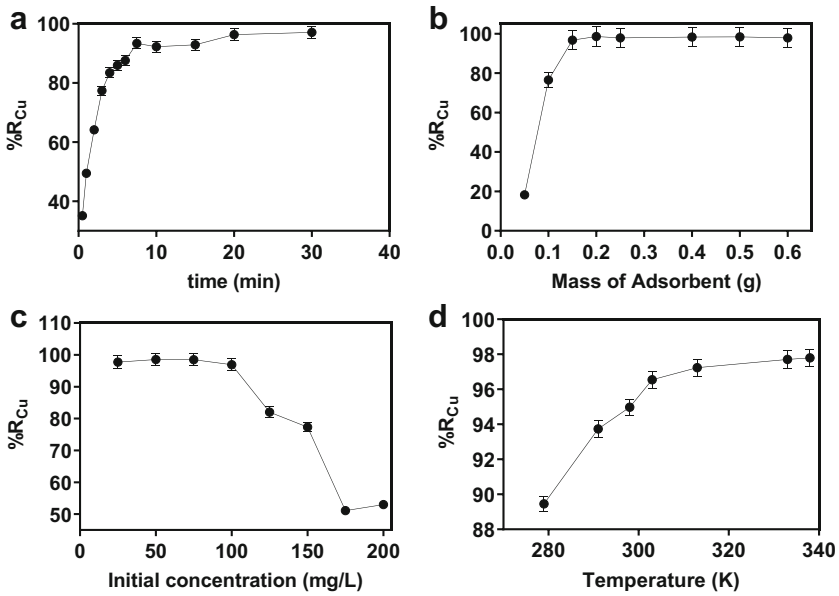

Fig. 4 **a** Effect of contact time (t_c) on the $\%R_{Cu}$ by TRH. **b** Effect of adsorbent dosage (D_{ad}) on the $\%R_{Cu}$ by TRH. **c** Effect of initial Cu (II) concentration ($[Cu]_i$) on the $\%R_{Cu}$ by TRH. **d** Effect of temperature (T) on the $\%R_{Cu}$ by TRH

Fomina and Gadd [25] reported an improvement in heavy metal removal by increasing D_{ad} to a certain limit due to the filling up of active sites via adsorbed metal. Lee and Chang [57] showed that heavy metal removal is indirectly related to the D_{ad}. Thus, the removal rate decreases by increasing the D_{ad}, whereas the work of Bhatti et al. [14] suggested that increasing the D_{ad} decreases the percentage removal of heavy metals. It was also proposed that the interference between the adsorbent sites with one another resulted in intracellular electrostatic interactions and reduced the percentage of heavy metal removals. The attraction between adsorbent and heavy metal was examined by FTIR and revealed that metals are attached to the peaks related to OH, N–H, and S=O. The obtained results suggest that Cu was successfully attached to the TRH surface via electrostatic force after the ion exchange of H^+ with water [6, 23].

3.2.3 Effect of initial Cu (II) concentration ($[Cu]_i$)

The effect of $[Cu]_i$ on the $\%R_{Cu}$ is depicted in Fig. 4c. At the low $[Cu]_i$, the number of active sites is higher than the $[Cu]_i$ and the $\%R_{Cu}$ was high, while at high $[Cu]_i$ the concentration of active sites is limited and will be filled fast leading to a notable decrease in the $\%R_{Cu}$. The $\%R_{Cu}$ was decreased from 97.5 to 55% as the $[Cu]_i$ increased from 25 to 175 mg L^{-1}. The obtained trends were related to the saturation of *ads* active sites, leaving some of the metal ions unabsorbed at higher $[Cu]_i$. Similar results were reported by various researchers [47, 93, 108, 113, 114].

3.2.4 Effect of temperature (T)

The effect of T on the $\%R_{Cu}$ from aqueous solution by TRH was investigated using the optimized conditions and presented in Fig. 4d. There was an increase in the $\%R_{Cu}$ by increasing the T, which indicates higher *ads* capacity at elevated temperatures. The $\%R_{Cu}$ increased by increasing the operating temperature from 279 to 338 K. The observed trends can be either due to the acceleration of some originally slow *ads* steps or to the creation of some new active sites on the surface of the sorbent. Moreover, the obtained behaviors can be related to the fact that at higher T will provide the required energy for the rate-determining of the chemisorption mechanisms allowing Cu to reach new active sites and enhance the removal efficiency [39, 40]. Zafar et al. [113] observed similar results during the removal of cerium ions from aqueous solution using rice husk. Khan et al. [46] used *Citrus sinensis* leaves and *Morus alba* leaves for the removal of Congo red dye from aqueous solution and reported comparable results. The capacity of the TRH showed higher capacity compared with other adsorbents from literature as shown in Table 1.

3.3 Adsorption kinetics

The nonlinear plots of PFO and PSO kinetic models for the *ads* of Cu (II) are represented in Fig. 5. Linear forms of the PFO (Fig. 6a) and PSO (Fig. 6b) following Eqs. (4) and (5) were used to determine the corresponding kinetic and equilibrium constants as shown in Table 2. The calculated values of R^2 for linear equations and χ^2 values for nonlinear equations are shown in Table 2. Results show that the PSO fits well the *ads* Cu on TRH with R^2 of 0.99 compared with PFO (R^2 = 0.75).

Table 1 *Ads* capacity of Cu (II) for different adsorbents

Adsorbent	Capacity (mg g^{-1})	References
N(2-Carboxybenzyl) grafted chitosan	0.027	[53]
Chitosan–GLA beads	6.210	[74]
Chitosan beads	21.55	[74]
Chitosan–alginate beads	27.44	[74]
Activated carbon	540.14	[87]
Untreated fruit peel	0.137	[95]
Treated fruit peel	0.486	[95]
Palm nut	2.667	[77]
Chestnut	3.247	[110]
Palm shell activated carbon	0.228	[80]
Coconut husk	0.668	[1]
Low-cost mineral	33.18	[84]
Sludge pyrolysis	0.620	[103]
Modified *Gmelina arborea* leaves	3.971	[101]
Gmelina arborea leaves	5.176	[101]
Activated carbon from *Ceiba pentandra* hulls	9.060	[68]
Rice bran	7.130	[106]
Sawdust	1.347	[56]
Dehydrated wheat bran	14.10	[81]
Cone biomass	5.110	[76]
Chitosan/sisal/banana fiber hybrid composite	1.885	[12]
Treated rice husk	48.841	Present study

Similarly, a small value of χ^2 of the PSO kinetic model indicates that PSO model seems to be more suitable to predict the kinetic parameter of Cu(II) *ads* onto TRH, and the PFO kinetic is not an appropriate model to explain the kinetic data of copper ion *ads* onto TRH. The data in Table 2 show that the percentage of error for the PFP is greater than PSO conforming that the PSO fits better the *ads* kinetic of Cu on TRH. The values of the K_2 constant show excellent and fast Cu *ads* kinetics compared with the data published on similar systems as reported by Khan et al. [42].

3.4 Adsorption isotherms

The experimental results were tested against Langmuir, Freundlich, and Dubinin–Radushkevich isotherms. These isotherms were widely used for the analysis and design of the *ads* process and scale-up to commercial level. Besides, the isotherms provide fundamental data about the applicability of the process as a unit operation. Langmuir isotherm has been used by various workers for the *ads* study of a variety of systems [54]. Langmuir model supposes homogeneity of the adsorbing surface, no interactions between adsorbed species, and no transmigration of adsorbate species in the plane of the surface. The difference in *ads* capacities of two adsorbents for the same adsorbate is believed to be largely due to their physicochemical properties or the chemistry of solution containing adsorbing species. In general, Q_{max} and K_L are functions of pH, ionic media, and ionic strength. The value of Q_{max} for Cu (II) was computed following the Langmuir isotherm using Wavemetrices IGOR Pro 6.1.2 software. A representative plot

Table 2 PFP and PSO kinetic parameters of the *ads* of Cu on TRH

Model	Rate constant (k) k_1 (min^{-1}) k_2 (g mg^{-1} min^{-1})	Q_e (mg g^{-1})	% Error	χ^2	R^2
PFO nonlinear	0.764	3.326	6.838	0.187	
PFO linear	0.227	1.634	54.227		0.75
PSO nonlinear	0.277	3.749	−5.032	0.069	
PSO linear	0.342	3.615	−4.046		0.99
Experimental Q_e	= 3.570 (mg g^{-1})				

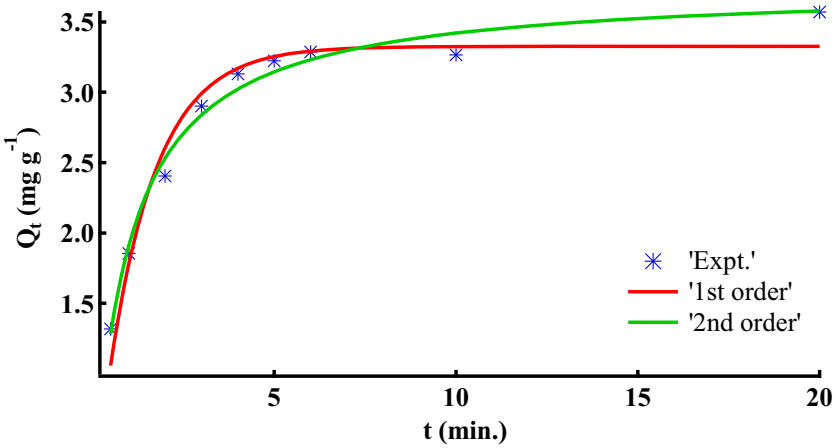

Fig. 5 Nonlinear plots of pseudo-first-order and pseudo-second-order kinetics models for the *ads* of Cu (II) onto TRH

of the linearized form of the Langmuir isotherm model for *ads* of Cu (II) onto TRH is represented in Fig. 7a. The corresponding equilibrium constants are given in Table 3. An essential feature of a Langmuir isotherm can be expressed in terms of a dimensionless constant "separation factor" parameter, R_L, that is used to predict if an *ads* system is "favorable" or "unfavorable" and can be expressed as in Eq. (16):

$$R_L = \frac{1}{\left(1 + k_L[Cu]_i\right)} \tag{16}$$

where $[Cu]_i$ is the initial concentration of Cu (mol $L^{-}1$) and K_L is the Langmuir sorption equilibrium constant (L mol^{-1}). The value of R_L indicates if the *ads* process is either unfavorable ($R_L > 1$), linear ($R_L = 1$), favorable ($0 < R_L < 1$), or irreversible ($R_L = 0$). Langmuir *ads* process deals with the formation of a monolayer of Cu on the surface of the TRH, and afterward, no further *ads* take place. The values of R_L for *ads* of Cu (II) was calculated from Langmuir constant K_L and initial concentrations of metal ion and results are summarized in Table 3, which confirmed that the *ads* of Cu (II) onto TRH was favorable as indicated by the fractional values of R_L between one and zero.

Freundlich isotherm assumes an exponentially decay in the density of the active site concerning the heat of *ads*. In this sense, Freundlich isotherms can be used as an indicator of the heterogeneity of the adsorbent surface. The constants in Freundlich isotherms (K_f and n) represents the *ads* capacity and intensity, respectively. Fitting of the experimental data (Fig. 7b) to Freundlich isotherm suggests that this isotherm is not suitable to represent the *ads* of Cu on TRH, and the corresponding isotherm parameters are given in Table 3. The value of n signifies the heterogeneous surface of the TRH. The values of n in the range 2–10 indicating good *ads* capacity, 1–2 as moderate *ads* capacity, and less than 1 as poor *ads* capacity [98, 115, 116]. The linearized form of D-R isotherm is given in Eq. (10). From β value, the mean *ads* energy (E) can be computed as in Eq. (17) [35]:

$$E = \frac{1}{\sqrt{-2\beta}} \tag{17}$$

which is the mean free energy of transfer of one mole of solute from infinity to the surface of the adsorbent. The plots of straight lines were obtained by using the linear form of D-R isotherm of Eq. (17) and are presented in Fig. 7c. The values of C_{max} and β were calculated from intercepts and slopes of the plot of $\ln\{q_e\}$ vs. ε^2 using a least-square fit program and are presented in Table 3. The D-R constants (C_{max}) for *ads* of Cu (II) onto TRH was evaluated from the intercept of straight lines using the least square fit program to be (1.9514 ± 0.477)

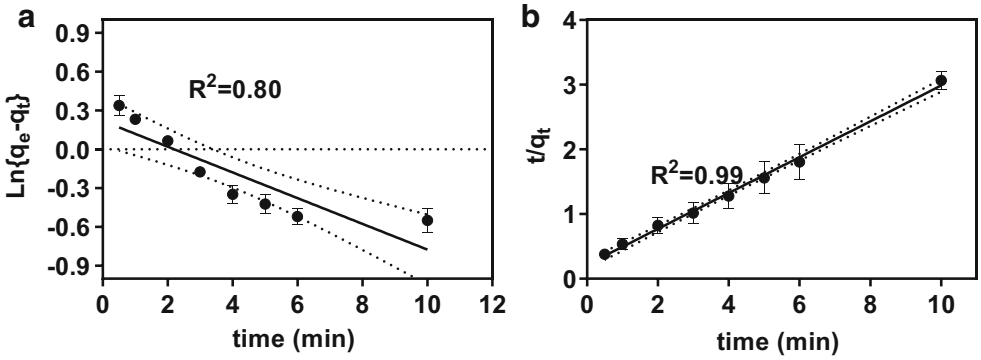

Fig. 6 **a** Linear plot of pseudo-first-order for *ads* of Cu (II) onto TRH and **b** linear plot of pseudo-second-order for *ads* of Cu (II) onto TRH

Table 3 Langmuir, Freundlich, and Dubinin–Radushkevivh isotherms parameters

Isotherms	Parameters		χ^2
Langmuir isotherm	Q_{max}	K_L	0.99
	9.17×10^{-5}	55,340 + 5234	
Freundlich isotherm	K_F	n	
	$(6.255 \pm 2.460) \times 10^{-4}$	4.351 ± 0.580	0.65
D-R isotherm	C_m	β	
	$(1.9514 \pm 0.477) \times 10^{-4}$	$(2.105 \pm 0.544) \times 10^{-3}$	0.68
		$E = 16.64 \pm 5.016$	

$\times 10^{-4}$. Using a β value of $(2.105 \pm 0.544) \times 10^{-3}$, the *ads* free energy (E) was calculated to be 14.43 ± 4.885 kJ mol^{-}1. The high numerical values of E suggest that the chemisorption phenomenon between Cu (II) and TRH is well established with a strong bond.

3.5 Adsorption thermodynamics study

The feasibility and spontaneity of the *ads* process were investigated by performing thermodynamic tests following Eqs. (11) and (12). The plot of $\ln K_c$ vs. $1/T$ for the *ads* of Cu onto TRH is depicted in Fig. 7d. The values of ΔH^o and S^o were calculated from the slope and intercept of Fig. 7d and are shown in Table 4. On the other hand, ΔG^o was also measured from Eq. (21) and is represented in Table 4. The values of ΔG^o decrease by increasing the T representing a decrease in the required T to achieve high $\%R_{Cu}$. Furthermore, the negative values of ΔG^o for the *ads* of Cu (II) onto TRH show that the *ads* process is spontaneous. The positive value of H^o depicts that the *ads* of Cu (II) onto TRH is an endothermic process. Similarly, the positive value of S^o represents the enhancement in randomness at the adsorbent–adsorbate interface during the sorption of Cu (II) onto TRH.

3.6 Recovery of Cu (II) and recycling the TRH

A series of experiments were performed with varying concentrations of acid solutions for the desorption of Cu (II) from TRH. Among the several acid solutions, HNO_3 solution gave maximum recovery of Cu (II) (~99%) with 1.0 mol L^{-1}. On the other hand, the recovery of Cu (II) from TRH was lower for an aqueous solution of HCl (1.0 mol L^{-1}) and H_2SO (1.0 mol L^{-1}). The lower concentration of HCl and H_2SO_4 was used because their higher concentration might damage the active site on the TRH. The obtained result was consistent with the phenomena explained in the effect of acid concentration that the *ads* process was decreased with an increase in the concentration of acids. As indicated above that Cu is attached to the TRH surface via

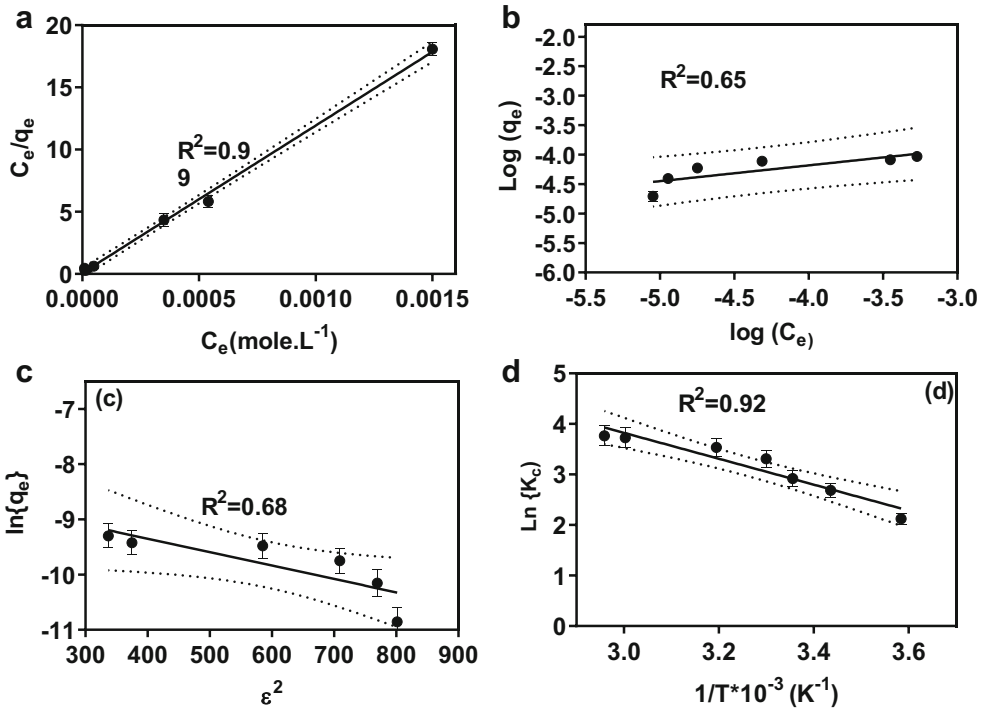

Fig. 7 **a** Linear form of Langmuir isotherm for *ads* of Cu (II) onto TRH. **b** Linear form of Freundlich isotherm for *ads* of Cu (II) onto TRH. **c** Linear form of Dubinin–Radushkevich (D-R) isotherm for *ads* of Cu (II) onto TRH. **d** Plot of $1/T$ vs. $\ln K_c$ for *ads* of Cu (II) onto TRH

Table 4 Thermodynamic parameters for *ads* of Cu (II) onto TRH

Temperature (K)	ΔH (KJ mol^{-}1)	ΔS (J mol^{-}1)	ΔG (KJ mol^{-1})
273			−26.15
291			−27.87
298			−28.54
303	21.33	95.84	−29.02
313			−29.98
333			−31.90
338			−32.38

electrostatic force after ion exchange of H^+ [6, 23]. Acid likely plays an important role in the regeneration or recovery of Cu from TRH. Another set of experiments was carried out to determine the number of cycles the TRH can be used for the removal of Cu. Results showed that the $\%R_{Cu}$ did not significantly change for 10 cycles. The reductions in $\%R_{Cu}$ after 5, 8, and 10 cycles were no more than 4, 7, and 9%, respectively, suggesting a reasonable service life and good *ads* capacity.

4 Conclusions

Herein, the batch removal of Cu (II) by TRH from aqueous solution was studied. The percentage removal of Cu (II) was increased by increasing the C_t, D_{Ad}, and T, whereas it decreased by increasing the $[Cu]_i$. Chemical treatment improved the surface properties of the RH, increased the negative functional groups and enhanced Cu removals by 1.8 compared with untreated RH. Electrostatic interaction force controls the main mechanism between algae strains and HM. The *ads* of Cu on TRH is endothermic and spontaneous and well fitted into the pseudo-second-order kinetic and Langmuir isotherm. Furthermore, the recovery of Cu (II) was maximum for HNO_3 (1.0 mol L^{-1}) solution suggesting that the TRH could be used as an excellent and cheap adsorbent for removal of Cu (II) from aqueous solution at room temperature.

Acknowledgment The authors are highly thankful to the Higher Education Commission (HEC), Pakistan for their financial support.

Funding Open Access funding provided by the Qatar National Library.

Nomenclature C_o, Initial concentration of Cu (II) (mg L^{-1}); C_t, Concentration of Cu (II) at time t (mg L^{-1}); W, Weight of adsorbent (g); V, Volume of adsorbate (dm^3); k_1, *Rate constant of pseudo-first-order model* (min^{-1}); k_2, *Rate constant of pseudo-second-order model* (g mg^{-1} min^{-1}); α, *Initial sorption rate* (mg g^{-1} min^{-1}); β, Extent *of surface coverage and activation energy for the chemisorption* (g mg^{-1}); K_{fd}, *Liquid film diffusion rate constant*; k, *Apparent* sorption *rate constant* (L g^{-1} min^{-1}); m, *Kuo–Lotse constant*; K_L, *Langmuir constant* (L mg^{-1}); q_m, *Langmuir monolayer* sorption *capacity* (mg g^{-1}); K_f, Freundlich constant; T, *Absolute temperature (K)*; R, *Gas constant (8.31 J* mol^{-1} K^{-1}); $\Delta G°$, Change in Gibb's energy; $\Delta S°$, Change in entropy; $\Delta H°$, Change in enthalpy

References

1. Abdulrasaq OO, Basiru OG (2010) Removal of copper (II), iron (III) and lead (II) ions from mono-component simulated waste effluent by *Ads* on coconut husk. Afr. J. Environ. Sci. Technol. 4
2. Ahmad RFK (2014) Kinetics, thermodynamics and adsorption of BTX via date-palm pits carbonization I aqueous solution.
3. Z. Aksu, İ.A. İşoğlu, Removal of copper(II) ions from aqueous solution by biosorption onto agricultural waste sugar beet pulp. Process Biochem. **40**, 3031–3044 (2005). https://doi.org/10.1016/j.procbio.2005.02.004
4. M.A. Al-Anber, Z.A. Al-Anber, I. Al-Momani, F. Al-Momani, Q. Abu-Salem, The performance of defatted jojoba seeds for the removal of toxic high concentration of the aqueous ferric ion. Desalin. Water Treat. **52**, 293–304 (2014). https://doi.org/10.1080/19443994.2013.784878
5. I. Ali, V.K. Gupta, Advances in water treatment by adsorption technology. Nat. Protoc. **1**, 2661–2667 (2006). https://doi.org/10.1038/nprot.2006.370
6. Almomani F, Bhosale R, Khraisheh M, Almomani T (2019) Heavy metal ions removal from industrial wastewater using magnetic nanoparticles (MNP). Appl. Surf. Sci. 144924
7. A.M.D. Al Ketife, F. Al Momani, S. Judd A bioassimilation and bioaccumulation model for the removal of heavy metals from wastewater using algae: New strategy Process Safety and Environmental Protection **144**, 52–64 (2020)
8. T. Aman, A.A. Kazi, M.U. Sabri, Q. Bano, Potato peels as solid waste for the removal of heavy metal copper(II) from waste water/industrial effluent. Colloids Surf. B: Biointerfaces **63**, 116–121 (2008). https://doi.org/10.1016/j.colsurfb.2007.11.013
9. T.G. Asere, C.V. Stevens, G. Du Laing, Use of (modified) natural adsorbents for arsenic remediation: a review. Sci. Total Environ. **676**, 706–720 (2019). https://doi.org/10.1016/j.scitotenv.2019.04.237
10. H. Aydın, Y. Bulut, Ç. Yerlikaya, Removal of copper (II) from aqueous solution by adsorption onto low-cost adsorbents. J. Environ. Manag. **87**, 37–45 (2008). https://doi.org/10.1016/j.jenvman.2007.01.005
11. N. Bakhtiari, S. Azizian, S.M. Alshehri, N.L. Torad, V. Malgras, Y. Yamauchi, Study on adsorption of copper ion from aqueous solution by MOF-derived nanoporous carbon. Microporous Mesoporous Mater. **217**, 173–177 (2015). https://doi.org/10.1016/j.micromeso.2015.06.022
12. L.K. Bakiya, P.N. Sudha, Adsorption of copper (II) ion onto chitosan/sisal/banana fiber hybrid composite. Int. J. Environ. Sci. **3**, 453–470 (2012)
13. C.E.R. Barquilha, E.S. Cossich, C.R.G. Tavares, E.A. da Silva, Biosorption of nickel and copper ions from synthetic solution and electroplating effluent using fixed bed column of immobilized

brown algae. J. Water Process. Eng. **32**, 100904 (2019). https://doi.org/10.1016/j.jwpe.2019.100904
14. H.N. Bhatti, A.W. Nasir, M.A. Hanif, Efficacy of Daucus carota L. waste biomass for the removal of chromium from aqueous solutions. Desalination **253**, 78–87 (2010). https://doi.org/10.1016/j.desal.2009.11.029
15. T. Bohli, I. Villaescusa, A. Ouederni, Comparative study of bivalent cationic metals adsorption Pb (II), Cd (II), Ni (II) and Cu (II) on olive stones chemically activated carbon. Chem. Eng. Process Technol. **4**, 1–7 (2013)
16. L. Castro, M.L. Blázquez, F. González, J.A. Muñoz, A. Ballester, Biosorption of Zn(II) from industrial effluents using sugar beet pulp and F. vesiculosus: from laboratory tests to a pilot approach. Sci. Total Environ. **598**, 856–866 (2017). https://doi.org/10.1016/j.scitotenv.2017.04.138
17. H. Chen, G. Dai, J. Zhao, A. Zhong, J. Wu, H. Yan, Removal of copper(II) ions by a biosorbent—Cinnamomum camphora leaves powder. J. Hazard. Mater. **177**, 228–236 (2010). https://doi.org/10.1016/j.jhazmat.2009.12.022
18. S.Y. Cheng, P.-L. Show, B.F. Lau, J.-S. Chang, T.C. Ling, New prospects for modified algae in heavy metal adsorption. Trends Biotechnol. **37**, 1255–1268 (2019). https://doi.org/10.1016/j.tibtech.2019.04.007
19. A. Cherfi, M. Achour, M. Cherfi, S. Otmani, A. Morsli, Health risk assessment of heavy metals through consumption of vegetables irrigated with reclaimed urban wastewater in Algeria. Process Saf. Environ. Prot. **98**, 245–252 (2015). https://doi.org/10.1016/j.psep.2015.08.004
20. A. Demirbas, Heavy metal adsorption onto agro-based waste materials: a review. J. Hazard. Mater. **157**, 220–229 (2008). https://doi.org/10.1016/j.jhazmat.2008.01.024
21. R. Djeribi, O. Hamdaoui, Sorption of copper(II) from aqueous solutions by cedar sawdust and crushed brick. Desalination **225**, 95–112 (2008). https://doi.org/10.1016/j.desal.2007.04.091
22. M. Dundar, C. Nuhoglu, Y. Nuhoglu, Biosorption of Cu(II) ions onto the litter of natural trembling poplar forest. J. Hazard. Mater. **151**, 86–95 (2008). https://doi.org/10.1016/j.jhazmat.2007.05.055
23. K. El-Boubbou, C. Gruden, X. Huang, Magnetic glyco-nanoparticles: a unique tool for rapid pathogen detection, decontamination, and strain differentiation. J. Am. Chem. Soc. **129**, 13392–13393 (2007)
24. A. Florido, C. Valderrama, J.A. Arévalo, I. Casas, M. Martínez, N. Miralles, Application of two sites non-equilibrium sorption model for the removal of Cu (II) onto grape stalk wastes in a fixed-bed column. Chem. Eng. J. **156**, 298–304 (2010)
25. M. Fomina, G.M. Gadd, Biosorption: current perspectives on concept. Definition Appl. Bioresour. Technol. **160**, 3–14 (2014). https://doi.org/10.1016/j.biortech.2013.12.102
26. F. Fu, Q. Wang, Removal of heavy metal ions from wastewaters: a review. J. Environ. Manag. **92**, 407–418 (2011). https://doi.org/10.1016/j.jenvman.2010.11.011
27. Y. Fu, Y. Shen, Z. Zhang, X. Ge, M. Chen, Activated bio-chars derived from rice husk via one- and two-step KOH-catalyzed pyrolysis for phenol adsorption. Sci. Total Environ. **646**, 1567–1577 (2019)
28. R. Gündoğan, B. Acemioğlu, M.H. Alma, Copper (II) adsorption from aqueous solution by herbaceous peat. J. Colloid Interface Sci. **269**, 303–309 (2004). https://doi.org/10.1016/S0021-9797(03)00762-8
29. J. He, J.P. Chen, A comprehensive review on biosorption of heavy metals by algal biomass: materials, performances, chemistry, and modeling simulation tools. Bioresour. Technol. **160**, 67–78 (2014). https://doi.org/10.1016/j.biortech.2014.01.068
30. Y.-S. Ho, Effect of pH on lead removal from water using tree fern as the sorbent. Bioresour. Technol. **96**, 1292–1296 (2005)
31. Y.-S. Ho, G. McKay, Pseudo-second order model for sorption processes. Process Biochem. **34**, 451–465 (1999)
32. Y.S. Ho, C.T. Huang, H.W. Huang, Equilibrium sorption isotherm for metal ions on tree fern. Process Biochem. **37**, 1421–1430 (2002). https://doi.org/10.1016/S0032-9592(02)00036-5
33. J. Igwe, A. Abia, Adsorption kinetics and intraparticulate diffusivities for bioremediation of Co (II), Fe (II) and Cu (II) ions from waste water using modified and unmodified maize cob. Int. J. Physical Sci. **2**, 119–127 (2007)
34. M. Iqbal, A. Saeed, S.I. Zafar, FTIR spectrophotometry, kinetics and adsorption isotherms modeling, ion exchange, and EDX analysis for understanding the mechanism of Cd2+ and Pb2+ removal by mango peel waste. J. Hazard. Mater. **164**, 161–171 (2009)
35. A. Itodo, H. Itodo, Sorption energies estimation using Dubinin–Radushkevich and Temkin adsorption isotherms. Life Sci. J-Acta Zhengzhou Univ. **7**, 31–39 (2010)
36. J. Jang, W. Miran, S.D. Divine, M. Nawaz, A. Shahzad, S.H. Woo, D.S. Lee, Rice straw-based biochar beads for the removal of radioactive strontium from aqueous solution. Sci. Total Environ. **615**, 698–707 (2018)
37. S. Kazy, K. Sar, P. Sen, A.K. Singh, S. FDS, Extracellular polysaccharides of a copper sensitive and a copper resistant Pseudomonas aeruginosa stain: synthesis, chemical nature and copper binding. W J Microbiol Biotechnol **18**, 583–588 (2002)
38. S.K. Kazy, S. D'Souza, P. Sar, Uranium and thorium sequestration by a Pseudomonas sp.: mechanism and chemical characterization. J. Hazard. Mater. **163**, 65–72 (2009)
39. N. Khalid, S. Ahmad, S.N. Kiani, J. Ahmed, Removal of lead from aqueous solutions using rice husk. Sep. Sci. Technol. **33**, 2349–2362 (1998)
40. N. Khalid, S. Ahmad, S.N. Kiani, J. Ahmed, Removal of mercury from aqueous solutions by adsorption to rice husks. Sep. Sci. Technol. **34**, 3139–3153 (1999)
41. M.I. Khan, S. Akhtar, S. Zafar, A. Shaheen, M.A. Khan, R. Luque, Removal of Congo red from aqueous solution by anion exchange membrane (EBTAC). Adsorption Kinet. Themodyn. Mater. **8**, 4147–4161 (2015a)
42. M.I. Khan, S. Zafar, H.B. Ahmad, M. Hussain, Z. Shafiq, Use of Morus alba leaves as bioadsorbent for the removal of Congo red dye. Fresenius Environ. Bull. **24**, 2251–2258 (2015b)
43. M.A. Khan, M.I. Khan, S. Zafar, Removal of different anionic dyes from aqueous solution by anion exchange membrane. Membrane Water Treat. **8**, 259–277 (2016)
44. M.I. Khan, M.A. Khan, S. Zafar, M.N. Ashiq, M. Athar, A.M. Qureshi, M. Arshad, Kinetic, equilibrium and thermodynamic studies for the adsorption of methyl orange using new anion exchange membrane (BII). Desalin. Water Treat. **58**, 285–297 (2017a)
45. M.I. Khan, S. Zafar, M.A. Khan, A.R. Buzdar, P. Prapamonthon, Adsorption kinetic, equilibrium and thermodynamic study for the removal of Congo Red from aqueous solution. Desalin. Water Treat. **98**, 294–305 (2017b)
46. M.I. Khan, S. Zafar, A.R. Buzdar, M.F. Azhar, W. Hassan, A. Aziz, Use of citrus sinensis leaves as a bioadsorbent for removal of Congo red dye from aqueous solution. Fresenius Environ. Bull. **27**, 4679–4688 (2018a)
47. M.I. Khan, S. Zafar, M.A. Khan, F. Mumtaz, P. Prapamonthon, A.R. Buzdar, Bougainvillea glabra leaves for adsorption of Congo red from wastewater. Fresenius Environ. Bull. **27**, 1456–1465 (2018b)
48. M.I. Khan, S. Zafar, M.F. Azhar, A.R. Buzdar, W. Hassan, A. Aziz, M. Khraisheh, Leaves powder of syzgium cumini as an adsorbent for removal of Congo red dye from aqueous solution. Fresenius Environ. Bull. **27**, 3342–3350 (2018c)
49. M.I. Khan, T.M. Ansari, S. Zafar, A.R. Buzdar, M.A. Khan, F. Mumtaz, P. Prapamonthon, M. Akhtar, Acid green-25 removal

from wastewater by anion exchange membrane: adsorption kinetic and thermodynamic studies. Membrane Water Treat **9**, 79–85 (2018d)
50. M.I. Khan, M.H. Lashari, M. Khraisheh, S. Shahida, S. Zafar, P. Prapamonthon, A. ur Rehman, S. Anjum, N. Akhtar, F. Hanif, Adsorption kinetic, equilibrium and thermodynamic studies of Eosin-B onto anion exchange membrane. Desalin. Water Treat. **155**, 84–93 (2019)
51. B. Kızılkaya, G. Türker, R. Akgül, F. Doğan, Comparative study of biosorption of heavy metals using living green algae Scenedesmus quadricauda and Neochloris pseudoalveolaris: equilibrium and kinetics. J. Dispers. Sci. Technol. **33**, 410–419 (2012)
52. S. Kizito, S. Wu, W.K. Kirui, M. Lei, Q. Lu, H. Bah, R. Dong, Evaluation of slow pyrolyzed wood and rice husks biochar for adsorption of ammonium nitrogen from piggery manure anaerobic digestate slurry. Sci. Total Environ. **505**, 102–112 (2015)
53. G.Z. Kyzas, M. Kostoglou, N.K. Lazaridis, D.N. Bikiaris, N-(2-Carboxybenzyl) grafted chitosan as adsorptive agent for simultaneous removal of positively and negatively charged toxic metal ions. J. Hazard. Mater. **244-245**, 29–38 (2013). https://doi.org/10.1016/j.jhazmat.2012.11.049
54. I. Langmuir, The adsorption of gases on plane surfaces of glass, mica and platinum. J. Am. Chem. Soc. **40**, 1361–1403 (1918). https://doi.org/10.1021/ja02242a004
55. S. Largergren, Zur theorie der sogenannten adsorption geloster stoffe. Kungliga Svenska Vetenskapsakademiens Handlingar **24**, 1–39 (1898)
56. S. Larous, A.-H. Meniai, M.B. Lehocine, Experimental study of the removal of copper from aqueous solutions by adsorption using sawdust. Desalination **185**, 483–490 (2005a)
57. Y.-C. Lee, S.-P. Chang, The biosorption of heavy metals from aqueous solution by Spirogyra and Cladophora filamentous macroalgae. Bioresour. Technol. **102**, 5297–5304 (2011). https://doi.org/10.1016/j.biortech.2010.12.103
58. F. Li, X. Fang, Z. Zhou, X. Liao, J. Zou, B. Yuan, W. Sun, Adsorption of perfluorinated acids onto soils: kinetics, isotherms, and influences of soil properties. Sci. Total Environ. **649**, 504–514 (2019a)
59. M. Li, H. Liu, T. Chen, C. Dong, Y. Sun, Synthesis of magnetic biochar composites for enhanced uranium (VI) adsorption. Sci. Total Environ. **651**, 1020–1028 (2019b)
60. R. Liu, B. Lian, Non-competitive and competitive adsorption of Cd2+, Ni2+, and Cu2+ by biogenic vaterite. Sci. Total Environ. **659**, 122–130 (2019)
61. W.-C. Liu, S.-W. Chang, K.-T. Jiann, L.-S. Wen, K.-K. Liu, Modelling diagnosis of heavy metal (copper) transport in an estuary. Sci. Total Environ. **388**, 234–249 (2007). https://doi.org/10.1016/j.scitotenv.2007.08.011
62. L. Liu, W. Li, W. Song, M. Guo, Remediation techniques for heavy metal-contaminated soils: principles and applicability. Sci. Total Environ. **633**, 206–219 (2018). https://doi.org/10.1016/j.scitotenv.2018.03.161
63. B. Liu, N. Zhu, Y. Li, P. Wu, Z. Dang, Y. Ke, Efficient recovery of rare earth elements from discarded NdFeB magnets. Process Saf. Environ. Prot. **124**, 317–325 (2019). https://doi.org/10.1016/j.psep.2019.01.026
64. K. Low, C. Lee, S. Liew, Sorption of cadmium and lead from aqueous solutions by spent grain. Process Biochem. **36**, 59–64 (2000)
65. S. Lu, S.W. Gibb, Copper removal from wastewater using spent-grain as biosorbent. Bioresour. Technol. **99**, 1509–1517 (2008). https://doi.org/10.1016/j.biortech.2007.04.024
66. L. Ludueña, D. Fasce, V.A. Alvarez, P.M. Stefani, Nanocellulose from rice husk following alkaline treatment to remove silica. BioResources **6**, 1440–1453 (2011)
67. F. Luo, Y. Liu, X. Li, Z. Xuan, J. Ma, Biosorption of lead ion by chemically-modified biomass of marine brown algae Laminaria japonica. Chemosphere **64**, 1122–1127 (2006). https://doi.org/10.1016/j.chemosphere.2005.11.076
68. M. Madhava Rao, A. Ramesh, G. Purna Chandra Rao, K. Seshaiah, Removal of copper and cadmium from the aqueous solutions by activated carbon derived from Ceiba pentandra hulls. J. Hazard. Mater. **129**, 123–129 (2006)
69. U. Maheshwari, B. Mathesan, S. Gupta, Efficient adsorbent for simultaneous removal of Cu(II), Zn(II) and Cr(VI): kinetic, thermodynamics and mass transfer mechanism. Process Saf. Environ. Prot. **98**, 198–210 (2015). https://doi.org/10.1016/j.psep.2015.07.010
70. W.E. Marshall, M.M. Johns, Agricultural by-products as metal adsorbents: sorption properties and resistance to mechanical abrasion. J. Chem. Technol. Biotechnol: International Research in Process, Environmental AND Clean Technology **66**, 192–198 (1996)
71. M.A. Martín-Lara, N. Ortuño, J.A. Conesa, Volatile and semivolatile emissions from the pyrolysis of almond shell loaded with heavy metals. Sci. Total Environ. **613-614**, 418–427 (2018). https://doi.org/10.1016/j.scitotenv.2017.09.116
72. M. Mukhopadhyay, S.B. Noronha, G.K. Suraishkumar, Kinetic modeling for the biosorption of copper by pretreated Aspergillus niger biomass. Bioresour. Technol. **98**, 1781–1787 (2007). https://doi.org/10.1016/j.biortech.2006.06.025
73. S. Nekouei, F. Nekouei, I. Tyagi, S. Agarwal, V.K. Gupta, Mixed cloud point/solid phase extraction of lead(II) and cadmium(II) in water samples using modified-ZnO nanopowders. Process Saf. Environ. Prot. **99**, 175–185 (2016). https://doi.org/10.1016/j.psep.2015.11.005
74. W. Ngah, S. Fatinathan, Adsorption of Cu (II) ions in aqueous solution using chitosan beads, chitosan–GLA beads and chitosan–alginate beads. Chem. Eng. J. **143**, 62–72 (2008)
75. W.S.W. Ngah, M.A.K.M. Hanafiah, Biosorption of copper ions from dilute aqueous solutions on base treatedrubber (Hevea brasiliensis) leaves powder: kinetics, isotherm, and biosorption mechanisms. J. Environ. Sci. **20**, 1168–1176 (2008). https://doi.org/10.1016/S1001-0742(08)62205-6
76. Y. Nuhoglu, E. Oguz, Removal of copper (II) from aqueous solutions by biosorption on the cone biomass of Thuja orientalis. Process Biochem. **38**, 1627–1631 (2003)
77. J.T. Nwabanne, P.K. Igbokwe, Copper (II) uptake by adsorption using palmyra palm nut. Adv. Appl. Sci. Res. **2**, 166–175 (2011)
78. D.W. O'Connell, C. Birkinshaw, T.F. O'Dwyer, Heavy metal adsorbents prepared from the modification of cellulose: a review. Bioresour. Technol. **99**, 6709–6724 (2008). https://doi.org/10.1016/j.biortech.2008.01.036
79. A.E. Ofomaja, E.B. Naidoo, S.J. Modise, Removal of copper(II) from aqueous solution by pine and base modified pine cone powder as biosorbent. J. Hazard. Mater. **168**, 909–917 (2009). https://doi.org/10.1016/j.jhazmat.2009.02.106
80. Y.B. Onundi, A. Mamun, M. Al Khatib, Y. Ahmed, Adsorption of copper, nickel and lead ions from synthetic semiconductor industrial wastewater by palm shell activated carbon. Int. J. Environ. Sci. Technol. **7**, 751–758 (2010)
81. A. Özer, D. Özer, A. Özer, The adsorption of copper (II) ions on to dehydrated wheat bran (DWB): determination of the equilibrium and thermodynamic parameters. Process Biochem. **39**, 2183–2191 (2004)
82. F. Pinakidou, E. Kaprara, M. Katsikini, E.C. Paloura, K. Simeonidis, M. Mitrakas, Sn(II) oxy-hydroxides as potential adsorbents for Cr(VI)-uptake from drinking water: an X-ray absorption study. Sci. Total Environ. **551-552**, 246–253 (2016). https://doi.org/10.1016/j.scitotenv.2016.01.208

83. N. Prakash, P. Sudha, N. Renganathan, Copper and cadmium removal from synthetic industrial wastewater using chitosan and nylon 6. Environ. Sci. Pollut. Res. **19**, 2930–2941 (2012)
84. M. Prasad, H.-y. Xu, S. Saxena, Multi-component sorption of Pb (II), Cu (II) and Zn (II) onto low-cost mineral adsorbent. J. Hazard. Mater. **154**, 221–229 (2008)
85. Y. Prasanna Kumar, P. King, V.S.R.K. Prasad, Equilibrium and kinetic studies for the biosorption system of copper(II) ion from aqueous solution using Tectona grandis L.f. leaves powder. J. Hazard. Mater. **137**, 1211–1217 (2006). https://doi.org/10.1016/j.jhazmat.2006.04.006
86. B. Ramavandi, G. Asgari, Comparative study of sun-dried and oven-dried Malva sylvestris biomass for high-rate Cu(II) removal from wastewater. Process Saf. Environ. Prot. **116**, 61–73 (2018). https://doi.org/10.1016/j.psep.2018.01.012
87. X. Ren, J. Li, X. Tan, X. Wang, Comparative study of graphene oxide, activated carbon and carbon nanotubes as adsorbents for copper decontamination. Dalton Trans. **42**, 5266–5274 (2013). https://doi.org/10.1039/c3dt32969k
88. F. Sajadi, M.H. Sayadi, M. Hajiani, Study of optimizing the process of cadmium adsorption by synthesized silver nanoparticles using Chlorella vulgaris. J Birjand Univ Med Sci **23**, 119–129 (2016a)
89. M. Sarioglu, U.A. Güler, N. Beyazit, Removal of copper from aqueous solutions using biosolids. Desalination **239**, 167–174 (2009). https://doi.org/10.1016/j.desal.2007.03.020
90. A.R. Satayeva, C.A. Howell, A.V. Korobeinyk, J. Jandosov, V.J. Inglezakis, Z.A. Mansurov, S.V. Mikhalovsky, Investigation of rice husk derived activated carbon for removal of nitrate contamination from water. Sci. Total Environ. **630**, 1237–1245 (2018)
91. M.H. Sayadi, N. Salmani, A. Heidari, M.R. Rezaei, Bio-synthesis of palladium nanoparticle using Spirulina platensis alga extract and its application as adsorbent. Surf Interfaces **10**, 136–143 (2018). https://doi.org/10.1016/j.surfin.2018.01.002
92. M. Šćiban, M. Klašnja, B. Škrbić, Adsorption of copper ions from water by modified agricultural by-products. Desalination **229**, 170–180 (2008). https://doi.org/10.1016/j.desal.2007.08.017
93. Z. Shen, D. Hou, F. Jin, J. Shi, X. Fan, D.C. Tsang, D.S. Alessi, Effect of production temperature on lead removal mechanisms by rice straw biochars. Sci. Total Environ. **655**, 751–758 (2019)
94. S.R. Shukla, R.S. Pai, Adsorption of Cu(II), Ni(II) and Zn(II) on dye loaded groundnut shells and sawdust. Sep. Purif. Technol. **43**, 1–8 (2005). https://doi.org/10.1016/j.seppur.2004.09.003
95. C. Sirilamduan, C. Umpuch, P. Kaewsarn, Removal of copper from aqueous solutions by adsorption using modify Zalacca edulis peel modify. Songklanakarin J. Sci. Technol. **33**, 725–732 (2011)
96. S. Sobhanardakani, A. Jafari, R. Zandipak, A. Meidanchi, Removal of heavy metal (Hg(II) and Cr(VI)) ions from aqueous solutions using Fe2O3@SiO2 thin films as a novel adsorbent. Process Saf. Environ. Prot. **120**, 348–357 (2018). https://doi.org/10.1016/j.psep.2018.10.002
97. V.C. Srivastaa, I.D. Mall, I.M. Mishra, Characterization of mesoporous rice husk ash (RHA) and adsorption kinetics of metal ions from aqueous solution onto RHA. J. Hazard. Mater. **134**, 257–267 (2006)
98. B. Subramanyam, A. Das, Linearized and non-linearized isotherm models comparative study on adsorption of aqueous phenol solution in soil. Int. J. Environ. Sci. Technol. **6**, 633–640 (2009)
99. C.R. Teixeira Tarley, S.L. Costa Ferreira, M.A. Zezzi Arruda, Use of modified rice husks as a natural solid adsorbent of trace metals: characterisation and development of an on-line preconcentration system for cadmium and lead determination by FAAS. Microchem. J. **77**, 163–175 (2004). https://doi.org/10.1016/j.microc.2004.02.019
100. Y. Tian, M. Wu, R. Liu, Y. Li, D. Wang, J. Tan, R. Wu, Y. Huang, Electrospun membrane of cellulose acetate for heavy metal ion adsorption in water treatment. Carbohydr. Polym. **83**, 743–748 (2011). https://doi.org/10.1016/j.carbpol.2010.08.054
101. J.O. Tijani, Sorption of lead (II) and copper (II) ions from aqueous solution by acid modified and unmodified Gmelina arborea (Verbenaceae) leaves. J. Emerg. Trends Eng. Appl. Sci. (JETEAS) **2**, 734–740 (2011)
102. T. Townsend, T. Tolaymat, K. Leo, J. Jambeck, Heavy metals in recovered fines from construction and demolition debris recycling facilities in Florida. Sci. Total Environ. **332**, 1–11 (2004). https://doi.org/10.1016/j.scitotenv.2004.03.011
103. I. Velghe, R. Carleer, J. Yperman, S. Schreurs, J. D'Haen, Characterisation of adsorbents prepared by pyrolysis of sludge and sludge/disposal filter cake mix. Water Res. **46**, 2783–2794 (2012). https://doi.org/10.1016/j.watres.2012.02.034S0043-1354(12)00137-6
104. T. Wajima, A new carbonaceous adsorbent for heavy metal removal from aqueous solution prepared from paper sludge by sulfur-impregnation and pyrolysis. Process Saf. Environ. Prot. **112**, 342–352 (2017). https://doi.org/10.1016/j.psep.2017.08.033
105. Y. Wang, R. Liu, H2O2 treatment enhanced the heavy metals removal by manure biochar in aqueous solutions. Sci. Total Environ. **628-629**, 1139–1148 (2018). https://doi.org/10.1016/j.scitotenv.2018.02.137
106. X.-s. Wang, Y. Qin, Equilibrium sorption isotherms for of Cu^{2+} on rice bran. Process Biochem. **40**, 677–680 (2005)
107. X. Wang, L. Xia, K. Tan, W. Zheng, Studies on adsorption of uranium (VI) from aqueous solution by wheat straw. Environ. Prog. Sustain. Energy **31**, 566–576 (2012). https://doi.org/10.1002/ep.10582
108. G. Weigelhofer, E.-M. Pölz, T. Hein, Citizen science: how high school students can provide scientifically sound data in biogeochemical experiments. Freshwater Science **38**, 236–243 (2019)
109. J.Z. Xie, H.-L. Chang, J.J. Kilbane II, Removal and recovery of metal ions from wastewater using biosorbents and chemically modified biosorbents. Bioresour. Technol. **57**, 127–136 (1996)
110. Z.-Y. Yao, J.-H. Qi, L.-H. Wang, Equilibrium, kinetic and thermodynamic studies on the biosorption of Cu (II) onto chestnut shell. J. Hazard. Mater. **174**, 137–143 (2010)
111. X. Ying-Mei, Q. Ji, H. De-Min, W. Dong-Mei, C. Hui-Ying, G. Jun, Q.-M. Zhou, Preparation of amorphous silica from oil shale residue and surface modification by silane coupling agent. Oil Shale **27**, 37–46 (2010)
112. S. Zafar, M.I. Khan, M. Khraisheh, S. Shahida, N. Khalid, M.L. Mirza, Effective removal of lanthanum ions from aqueous solution using rice husk: impact of experimental variables. Desalin. Water Treat. **132**, 263–273 (2019a)
113. S. Zafar, M.I. Khan, M. Khraisheh, S. Shahida, T. Javed, M.L. Mirza, N. Khalid, Use of rice husk as an effective sorbent for the removal of cerium ions from aqueous solution: kinetic, equilibrium and thermodynamic studies. Desalin. Water Treat. **150**, 124–135 (2019b)
114. Q. Zhou, B. Liao, L. Lin, W. Qiu, Z. Song, Adsorption of Cu (II) and Cd (II) from aqueous solutions by ferromanganese binary oxide–biochar composites. Sci. Total Environ. **615**, 115–122 (2018)
115. Y. Zhou, Y. He, Y. He, X. Liu, B. Xu, J. Yu, C. Dai, A. Huang, Y. Pang, L. Luo, Analyses of tetracycline adsorption on alkali-acid modified magnetic biochar: site energy distribution consideration. Sci. Total Environ. **650**, 2260–2266 (2019a)
116. Y. Zhou, Y. He, Y. Xiang, S. Meng, X. Liu, J. Yu, J. Yang, J. Zhang, P. Qin, L. Luo, Single and simultaneous adsorption of pefloxacin and Cu (II) ions from aqueous solutions by oxidized multiwalled carbon nanotube. Sci. Total Environ. **646**, 29–36 (2019b)
117. C.-S. Zhu, L.-P. Wang, W.-B. Chen, Removal of Cu(II) from aqueous solution by agricultural by-product: peanut hull. J. Hazard. Mater. **168**, 739–746 (2009). https://doi.org/10.1016/j.jhazmat.2009.02.085